

Dynamical quantum phase transition in *XY* chains with the Dzyaloshinskii-Moriya and *XZY-YZY* three-site interactions

Kaiyuan Cao(曹凯源), Ming Zhong(钟鸣), and Peiqing Tong(童培庆)

Citation: Chin. Phys. B, 2022, 31 (**6**): 060505. DOI: 10.1088/1674-1056/ac4a6e
Journal homepage: http://cpb.iphy.ac.cn; http://iopscience.iop.org/cpb

What follows is a list of articles you may be interested in

Thermodynamic properties of two-dimensional charged spin-1/2 Fermi gases

Jia-Ying Yang(杨家营), Xu Liu(刘旭), Ji-Hong Qin(秦吉红), and Huai-Ming Guo(郭怀明)
Chin. Phys. B, 2022, 31 (**6**): 060504. DOI: 10.1088/1674-1056/ac4e0b

Topological Anderson insulator in two-dimensional non-Hermitian systems

Hongfang Liu(刘宏芳), Zixian Su(苏子贤), Zhi-Qiang Zhang(张智强), Hua Jiang(江华)
Chin. Phys. B, 2020, 29 (**5**): 050502. DOI: 10.1088/1674-1056/ab8201

Effect of system-reservoir correlations on temperature estimation

Wen-Li Zhu(朱雯丽), Wei Wu(吴威), Hong-Gang Luo(罗洪刚)
Chin. Phys. B, 2020, 29 (**2**): 020501. DOI: 10.1088/1674-1056/ab5fc0

Generalized Lanczos method for systematic optimization of tensor network states

Rui-Zhen Huang(黄瑞珍), Hai-Jun Liao(廖海军), Zhi-Yuan Liu(刘志远), Hai-Dong Xie(谢海东), Zhi-Yuan Xie(谢志远), Hui-Hai Zhao(赵汇海), Jing Chen(陈靖), Tao Xiang(向涛)
Chin. Phys. B, 2018, 27 (**7**): 070501. DOI: 10.1088/1674-1056/27/7/070501

Identifying the closeness of eigenstates in quantum many-body systems

Hai-bin Li(李海彬), Yang Yang(杨扬), Pei Wang(王沛), Xiao-guang Wang(王晓光)
Chin. Phys. B, 2017, 26 (**8**): 080502. DOI: 10.1088/1674-1056/26/8/080502

Dynamical quantum phase transition in XY chains with the Dzyaloshinskii–Moriya and XZY–YZX three-site interactions

Kaiyuan Cao(曹凯源)[1], Ming Zhong(钟鸣)[1], and Peiqing Tong(童培庆)[1,2,†]

[1] *Department of Physics and Institute of Theoretical Physics, Nanjing Normal University, Nanjing* 210023, *China*
[2] *Jiangsu Key Laboratory for Numerical Simulation of Large Scale Complex Systems, Nanjing Normal University, Nanjing* 210023, *China*

(Received 29 October 2021; revised manuscript received 19 December 2021; accepted manuscript online 12 January 2022)

We study the dynamical quantum phase transitions (DQPTs) in the XY chains with the Dzyaloshinskii–Moriya interaction and the XZY–YZX type of three-site interaction after a sudden quench. Both the models can be mapped to the spinless free fermion models by the Jordan–Wigner and Bogoliubov transformations with the form $H=\sum_k \varepsilon_k(\eta_k^\dagger \eta_k-\frac{1}{2})$, where the quasiparticle excitation spectra ε_k may be smaller than 0 for some k and are asymmetrical ($\varepsilon_k \neq \varepsilon_{-k}$). It is found that the factors of Loschmidt echo equal 1 for some k corresponding to the quasiparticle excitation spectra of the pre-quench Hamiltonian satisfying $\varepsilon_k \cdot \varepsilon_{-k} < 0$, when the quench is from the gapless phase. By considering the quench from different ground states, we obtain the conditions for the occurrence of DQPTs for the general XY chains with gapless phase, and find that the DQPTs may not occur in the quench across the quantum phase transitions regardless of whether the quench is from the gapless phase to gapped phase or from the gapped phase to gapless phase. This is different from the DQPTs in the case of quench from the gapped phase to gapped phase, in which the DQPTs will always appear. Moreover, we analyze the different reasons for the absence of DQPTs in the quench from the gapless phase and the gapped phase. The conclusion can also be extended to the general quantum spin chains.

Keywords: dynamical quantum phase transition, gapless phase, asymmetry excitation spectra

PACS: 05.30.–d, 75.10.Pq, 05.30.Rt **DOI:** 10.1088/1674-1056/ac4a6e

1. Introduction

Quantum phase transitions (QPTs) are one of the most significant phenomena in quantum many-body physics.[1,2] It is characterized by a nonanalytic behavior of some physical observable at a quantum critical point due to the change of the external control parameter. Recently, the dynamical quantum phase transitions (DQPTs) that in the quantum many-body systems have attracted extendedly both the theoretical[3–31] and experimental[32–37] interests. Unlike the QPTs driven by the external control parameters, the DQPTs describe the nonanalytic behavior of the Loschmidt echo (LE) during the time evolution, where a common protocol for driven a system out of equilibrium is called quantum quench. In many cases, the DQPTs are found to have a strong connection with the QPTs. The DQPTs are present in the cases of sudden quenches crossing the quantum critical points[3,4] and the topology changes,[5,8] although it is also found that the DQPTs occur in the cases of quenches without crossing any quantum critical point.[6,12] Therefore, it is still an open and debated issue whether the quench crossing the critical points of QPTs is a necessary condition to induce a DQPT.[22,27]

Up to now, many works have investigated the quench from gapped phase to gapped phase, whereas few studies have focused on the case of quench from the gapless phase. The gapless phase is of general existence in the quantum systems, such as the XY chain with the Dzyaloshinskii–Moriya (DM) interaction,[38–41] the XY chain with XZY–YZX type of three-site interactions[42,43] and Kitaev model.[44] Unlike the case of the gapped phase, the ground states of the system in the gapless phase corresponds to the configuration where all the states with negative excitation spectra are filled and nonnegative are empty.[45–47] Recently, Cheraghi and Mahdavifar studied the DQPTs in the quantum Ising chain with DM interaction.[16] They only considered the case of quench from gapped phase to gapped phase and did not consider the quench from the gapless phase, so that they concluded that the DM interaction does not affect the DQPT. In a recent paper,[27] the authors studied the DQPTs in the XY chain with DM interaction in the alternating external transverse field. They also did not discuss the case of quench starting from the gapless phase, because they said that it is difficult to study the initial condition in the gapless phase in their models.[27] Therefore, it is still unknown when the quench is from the gapless phase.

Recently, Jafari has studied the DQPTs in the extended XY chain with XZX+YZY type of three-site interaction in the staggered transverse field.[22] He found that the DQPTs may not occur when the quench is from the gapped phase to gapless phase. The model has the gapless phase due to the staggered external field and the quasiparticle excitation spectra are symmetrical.[22] In this paper, we investigate the DQPTs in the extended XY chains with DM interaction and XZY–YZX type of three site interactions. Both the models have asymmetrical quasiparticle excitation spectra ($\varepsilon_k \neq \varepsilon_{-k}$), which are different from the model in Ref. [22]. We study all possible situations of

†Corresponding author. E-mail: pqtong@njnu.edu.cn

© 2022 Chinese Physical Society and IOP Publishing Ltd

ground states of pre-quench Hamiltonian and obtain the general expression of LE for the systems with gapless phases (see Section 2). This allows our discussion to be generalized to the general quantum spin models. For the homogeneous system, the LE can be given by $\mathcal{L}(t)=\prod_{k>0}\mathcal{L}_k(t)$, where $\mathcal{L}_k(t)$ equals unity corresponding to the quasiparticle excitation spectra of pre-quench Hamiltonian satisfying $\varepsilon_k\cdot\varepsilon_{-k}<0$ in the momentum subspace $k>0$. Therefore, we obtain general conditions for the occurrence of DQPTs. In Sections 3 and 4, we discuss the behaviors of DQPTs for two extended XY chains by given numerical results. It is found that the DQPTs may not occur in the quench across the quantum phase transitions regardless of whether the quench is from the gapless phase to gapped phase or from gapped phase to gapless phase. A brief conclusion is given in Section 5.

2. Models and DQPT

We consider two kinds of the extended XY chains (with periodic boundary) in a transverse field: one with the added DM interaction and the other with added XZY–YZX type of three-site interaction. The Hamiltonian is written as

$$H=H_{XY}+H_{\rm add}, \tag{1}$$

with

$$H_{XY}=-\sum_{n=1}^{N}\left(\frac{1+\gamma}{2}\sigma_n^x\sigma_{n+1}^x+\frac{1-\gamma}{2}\sigma_n^y\sigma_{n+1}^y+h\sigma_n^z\right), \tag{2}$$

where $\sigma_n^{x,y,z}$ are the Pauli matrices, γ ($|\gamma|\leq 1$) is the anisotropic parameter, and h ($h>0$) is the external field. For the XY chains with DM interaction,[45,47]

$$H_{\rm add}=H_{\rm DM}=-\sum_{n=1}^{N}D(\sigma_n^x\sigma_{n+1}^y-\sigma_n^y\sigma_{n+1}^x), \tag{3}$$

where D is the strength of the DM interaction. For the XY chain with XZY–YZX type of three-site interaction,[42,48]

$$H_{\rm add}=H_{XZY-YZX}=\sum_{n=1}^{N}\frac{\xi}{4}(\sigma_{n-1}^x\sigma_n^z\sigma_{n+1}^y-\sigma_{n-1}^y\sigma_n^z\sigma_{n+1}^x)\}, \tag{4}$$

where ξ is the strength of the three-site interaction.

Both the models can be mapped to the spinless free fermion model via the Jordan–Wigner transformation, and can be written in the following quadratic form

$$H=\sum_{nm}c_n^\dagger A_{nm}c_m+\frac{1}{2}\sum_{nm}(c_n^\dagger B_{nm}c_m^\dagger+{\rm h.c.}), \tag{5}$$

where c_n and $c_n^\dagger$ are fermion annihilation and creation operators, respectively. Here, the fermion problem has the anti-periodic boundary condition for even N, and the periodic boundary condition for odd N. Then, by performing the Fourier transformation ($c_n=\sum_k c_k\,{\rm e}^{-{\rm i}kn}/\sqrt{N}$) and the Bogoliubov transformation ($\eta_k=u_kc_k+{\rm i}v_kc_{-k}^\dagger$),[2,46] we can obtain the diagonal Hamiltonian in the following form:

$$H=\sum_k\varepsilon_k\left(\eta_k^\dagger\eta_k-\frac{1}{2}\right), \tag{6}$$

where η_k and $\eta_k^\dagger$ are fermion annihilation and creation operators, and ε_k are the quasiparticle excitation spectra. For the XY chain with DM interaction, $\varepsilon_k=-4D\sin k+2\sqrt{(h+\cos k)^2+\gamma^2\sin^2 k}$. For the XY chain with XZY–YZX type of three-site interaction, $\varepsilon_k=\xi\sin 2k+2\sqrt{(h+\cos k)^2+\gamma^2\sin^2 k}$. Here we only consider the cases of $D<0.5$ for the XY chain with DM intersection and $\xi<1$ for the XY chain with XZY–YZX type of three-site interaction.

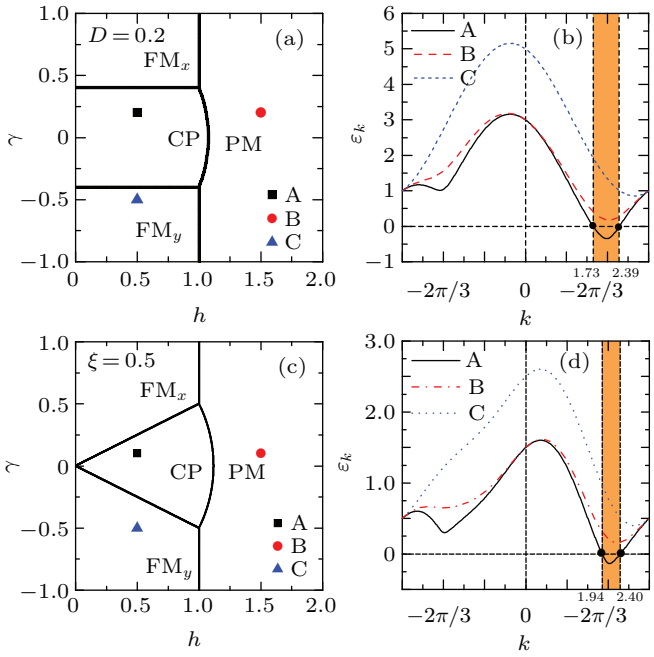


Fig. 1. (a) The typical phase diagram of the XY chain with DM interaction in the (h,γ) plane for $D=0.2$. (b) Three typical quasiparticle excitation spectra ε_k for points A, B, and C in (a). (c) The typical phase diagram of the XY chain with XZY–YZX type of three-site interaction for $\xi=0.5$. (d) Three typical ε_k for points A, B, and C in (a). Regions CP, PM, FM$_x$ and FM$_y$ between the solid lines correspond to the gapless chiral phase, gapped paramagnetic phase, gapped ferromagnetic phase along x direction and gapped ferromagnetic phase along y direction, respectively. The orange areas denote the negative quasiparticle excitation spectrum intervals ($\varepsilon_k<0$).

In Figs. 1(a) and 1(c), we show the phase diagrams in the (h–γ) plane for the XY chain with DM interaction ($D=0.2$)[47] and XZY–YZX type of three-site interaction ($\xi=0.5$),[48] respectively. Both the phase diagrams consist of four parts [see Figs. 1(a) and 1(c)]: gapless chiral (CP) phase, gapped paramagnetic (PM) phase, gapped ferromagnetic phase along x (FM$_x$) direction, and gapped ferromagnetic phase along y (FM$_y$) direction, where for gapless CP phase, $\varepsilon_k<0$ for some k, but for gapped phases, $\varepsilon_k>0$ for all k. In Figs. 1(b) and 1(d), we show three typical excitation spectra for points A, B, and C (see Figs. 1(a) and 1(c)) for the XY chain with DM interaction ($D=0.2$) and XZY–YZX type of three-site interaction

($\xi = 0.5$), respectively. The systems for points A are inside the gapless CP phase, and for points B and C are inside the gapped PM and FM$_y$ phases, respectively. It can be seen that ε_k are smaller than zero for some k when the systems are in the gapless CP phase.

According to Eq. (6), we have $H = \sum_{k>0} H_k$ with

$$\begin{aligned} H_k &= \varepsilon_k\left(\eta_k^\dagger\eta_k - \frac{1}{2}\right) + \varepsilon_{-k}\left(\eta_{-k}^\dagger\eta_{-k} - \frac{1}{2}\right) \\ &= \varepsilon_k\left(\hat{n}_k - \frac{1}{2}\right) + \varepsilon_{-k}\left(\hat{n}_{-k} - \frac{1}{2}\right), \end{aligned} \tag{7}$$

where $\hat{n}_k = \eta_k^\dagger\eta_k$ ($\hat{n}_{-k} = \eta_{-k}^\dagger\eta_{-k}$) is the number operator of the spinless fermion, and the corresponding eigenvalues are $n_k(n_{-k}) = 0, 1$. The ground states of the quasiparticles are determined by the quasiparticle excitation spectra, that is, for $\varepsilon_k > 0$, the ground states are empty ($\eta_k|GS\rangle = 0$), but for $\varepsilon_k < 0$, the ground states are filled ($\eta_k^\dagger|GS\rangle = 0$). Therefore, for these two models, the ground states can be expressed by

$$|GS\rangle = \begin{cases} \bigotimes_{k>0}|0_k 0_{-k}\rangle, & \text{PM, FM}_x\text{, and FM}_y, \\ \bigotimes_{k>0}|0_k 0_{-k}\rangle \bigotimes_{k'>0}|1_{k'} 0_{-k'}\rangle, & \text{CP}, \end{cases} \tag{8}$$

where $\varepsilon_k, \varepsilon_{-k} \geq 0$ and $\varepsilon_{k'} < 0$, $\varepsilon_{-k'} > 0$.

In a quantum quench, the system is prepared in the ground states of the Hamiltonian H. At time $t = 0$, the system undergoes a sudden quench with its Hamiltonian switched from H to $\widetilde{H}$. The Loschmidt amplitude is defined as (we take $\hbar = 1$)

$$\mathcal{G}(t) = \langle GS|\mathrm{e}^{\mathrm{i}Ht}\mathrm{e}^{-\mathrm{i}\widetilde{H}t}|GS\rangle = \mathrm{e}^{-\mathrm{i}(E_0-\widetilde{E}_0)t}\prod_{k>0}\mathcal{G}_k(t), \tag{9}$$

where $\mathcal{G}_k(t) = \langle n_k n_{-k}|\mathrm{e}^{-\mathrm{i}\widetilde{H}_k t}|n_k n_{-k}\rangle$, E_0 ($\widetilde{E}_0$) is the ground state energy of H ($\widetilde{H}$). To calculate the Loschmidt amplitude, we should expand the states $|n_k n_{-k}\rangle$ of the pre-quench Hamiltonian H_k by the eigenstates of the post-quench $\widetilde{H}_k$. Considering that both $\eta_k^\dagger$ and $\widetilde{\eta}_k^\dagger$ are related by the Bogoliubov transformation,[2,46] we can obtain the relations between the eigenstates of H_k and $\widetilde{H}_k$:

$$\begin{aligned} |0_k 0_{-k}\rangle &= \cos\alpha_k|\widetilde{0}_k\widetilde{0}_{-k}\rangle - \mathrm{i}\sin\alpha_k|\widetilde{1}_k\widetilde{1}_{-k}\rangle, \\ |1_k 0_{-k}\rangle &= |\widetilde{1}_k\widetilde{0}_{-k}\rangle, \\ |0_k 1_{-k}\rangle &= |\widetilde{0}_k\widetilde{1}_{-k}\rangle, \\ |1_k 1_{-k}\rangle &= -\mathrm{i}\sin\alpha_k|\widetilde{0}_k\widetilde{0}_{-k}\rangle + \cos\alpha_k|\widetilde{1}_k\widetilde{1}_{-k}\rangle, \end{aligned} \tag{10}$$

where $\alpha_k = \theta_k - \tilde{\theta}_k$, θ_k ($\tilde{\theta}_k$) are the Bogoliubov angles of the pre- and post-quench Hamiltonian. It should be noticed that $|1_k 0_{-k}\rangle$ and $|0_k 1_{-k}\rangle$ of the pre-quench Hamiltonian are also the eigenstates of the post-quench Hamiltonian $\widetilde{H}_k$.

Substituting Eq. (10) into Eq. (9), we can give the Loschmidt amplitudes $\mathcal{G}_k(t)$ as follows:

$$\mathcal{G}_k(t) = \begin{cases} \cos^2\alpha_k + \sin^2\alpha_k\,\mathrm{e}^{-\mathrm{i}t(\widetilde{\varepsilon}_k+\widetilde{\varepsilon}_{-k})}, & \varepsilon_k, \varepsilon_{-k} \geq 0, \\ \mathrm{e}^{-\mathrm{i}t(\widetilde{\varepsilon}_k+\widetilde{\varepsilon}_{-k})}, & \varepsilon_k < 0, \varepsilon_{-k} \geq 0, \\ \mathrm{e}^{-\mathrm{i}t(\widetilde{\varepsilon}_k+\widetilde{\varepsilon}_{-k})}, & \varepsilon_k \geq 0, \varepsilon_{-k} < 0, \\ \sin^2\alpha_k + \cos^2\alpha_k\,\mathrm{e}^{-\mathrm{i}t(\widetilde{\varepsilon}_k+\widetilde{\varepsilon}_{-k})}, & \varepsilon_k, \varepsilon_{-k} < 0. \end{cases} \tag{11}$$

Then, the LE reads

$$\mathcal{L}(t) = |\mathcal{G}(t)|^2 = \prod_{k>0}\mathcal{L}_k(t) \tag{12}$$

with

$$\mathcal{L}_k(t) = \begin{cases} 1 - \sin^2(2\alpha_k)\sin^2\left(\frac{\widetilde{\varepsilon}_k+\widetilde{\varepsilon}_{-k}}{2}t\right), & \varepsilon_k \cdot \varepsilon_{-k} \geq 0, \\ 1, & \varepsilon_k \cdot \varepsilon_{-k} \leq 0. \end{cases} \tag{13}$$

In order to show the DQPT more directly, one can use the dynamical free energy density, which is defined as the rate function $\lambda(t) = -\lim_{N\to\infty}\ln\mathcal{L}(t)/N$ of the LE. Analogous to the equilibrium phase transitions, the rate function will show the sharp nonanalyticities at the critical times of the DQPTs.[4] According to Eq. (13), the rate function of LE is

$$\lambda(t) = -\lim_{N\to\infty}\frac{1}{N}\sum_{k>0}\ln\mathcal{L}_k(t). \tag{14}$$

Obviously, for the cases of $\varepsilon_k \cdot \varepsilon_{-k} \leq 0$, $\ln\mathcal{L}_k(t) = 0$.

Another way to show the DQPTs is using the Fisher zeros of the Loschmidt amplitude in the complex time plane.[3,15] According to Eq. (11), for $\varepsilon_k \cdot \varepsilon_{-k} \leq 0$, $\mathcal{G}_k(z) = \mathrm{e}^{-z(\widetilde{\varepsilon}_k+\widetilde{\varepsilon}_{-k})}$ have no Fisher zeros in the complex time plane. Noticeably, for $\varepsilon_k \geq 0$ and $\varepsilon_{-k} \geq 0$, we can obtain the Fisher zeros z_n of the Loschmidt amplitude located on the lines ($n \in \mathbb{Z}$) as follows:

$$z_n(k) = \frac{1}{\widetilde{\varepsilon}_k + \widetilde{\varepsilon}_{-k}}[\ln\tan^2\alpha_k + \mathrm{i}\pi(2n+1)], \tag{15}$$

and for $\varepsilon_k < 0$ and $\varepsilon_{-k} < 0$

$$z_n(k) = \frac{1}{\widetilde{\varepsilon}_k + \widetilde{\varepsilon}_{-k}}[-\ln\tan^2\alpha_k + \mathrm{i}\pi(2n+1)]. \tag{16}$$

The DQPTs will occur if the Fisher zeros lines interacting with the imaginary axis. The imaginary parts of the Fisher zeros on the imaginary axis denote the critical times of the DQPTs. Therefore, the conditions for the occurrence of DQPTs are given by

$$|\tan\alpha_k| = 1, \tag{17}$$

$$\varepsilon_k \cdot \varepsilon_{-k} > 0. \tag{18}$$

If the above conditions (17) and (18) hold for a wave vector k^*, the corresponding critical times of the DQPTs are given by

$$t_n(k^*) = (2n+1)t_0(k^*), \tag{19}$$

where $t_0(k^*) = \frac{\pi}{\widetilde{\varepsilon}_{k^*}+\widetilde{\varepsilon}_{-k^*}}$, and k^* is the corresponding critical wave vectors.

3. The DQPT in the *XY* chain with DM interaction

For the quench from the $H(h_0, \gamma_0)$ to $H(h, \gamma)$, we define the domain $\mathcal{R}(h_0, \gamma_0)$ in the plane (h, γ), where the conditions (17) and (18) are satisfied. The domain $\mathcal{R}(h_0, \gamma_0)$ covers all the parameters of the post-quench Hamiltonian, in which the DQPT will occur for the quench from (h_0, γ_0). In the following, we discuss the cases of quenches from the gapless phase and the gapped phase, respectively.

3.1. Quench from the gapless phase

First, we consider the case of quench from the gapless phase. As a typical example, Fig. 2(a) shows the domain $\mathcal{R}(h_0 = 0.5, \gamma_0 = 0.2)$ for the quench from the gapless CP phase, where the domain is shown as the red region. It can be seen that the domain $\mathcal{R}(h_0 = 0.5, \gamma_0 = 0.2)$ does not cover all the areas of the PM, FM_x and FM_y phases, and also covers a part of the area in the CP phase. This means that the DQPT may occur for the quench within the gapless CP phase, and may not occur for the quench from the CP phase to the PM, FM_x and FM_y phases.

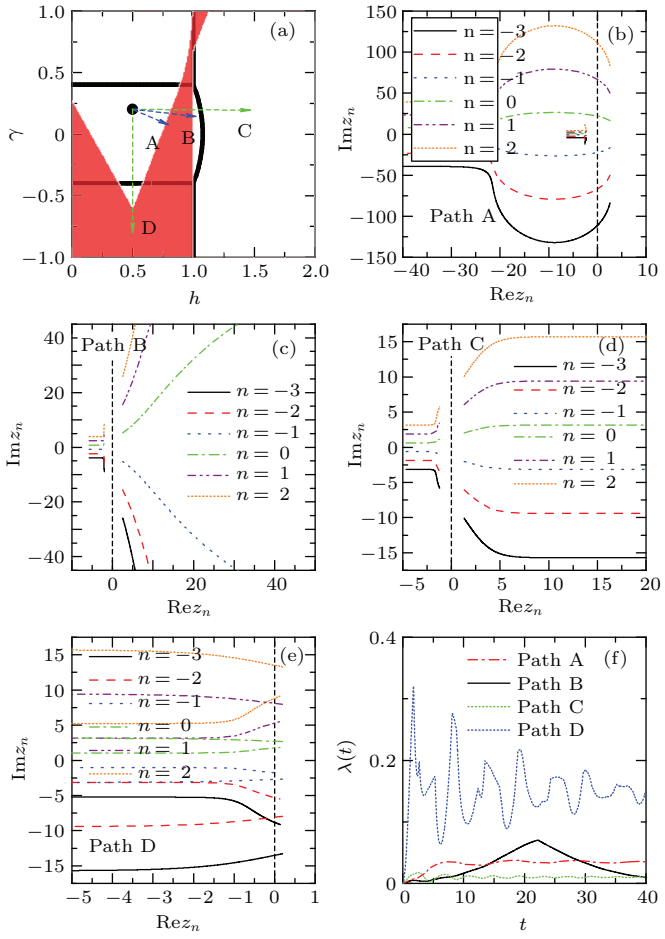


Fig. 2. (a) Domain $\mathcal{R}(h_0, \gamma_0)$ (the red region) covering the post-quench Hamiltonian parameters where the DQPTs appear for the quench from the initial points (h_0, γ_0). (b)–(e) The Fisher zeros for the quench paths A–D shown in (a). (f) The corresponding rate functions for the quench paths A–D.

To show the behaviors of DQPTs more clearly, we show four examples of the Fisher zeros $z_n(k)$ in Figs. 2(b)–2(e) for the quench paths A–D marked in Fig. 2(a), and the corresponding rate functions are given in Fig. 2(f). The paths A and B are within the CP phase, and the paths C and D are from the CP phase to the PM phase and FM_y phase, respectively. It should be noticed that all the Fisher zeros for the paths A–D are separated into two parts, because those wave vectors corresponding to $\varepsilon_k \cdot \varepsilon_{-k} < 0$ do not contribute to the Fisher zeros for the quench from the gapless CP phase. For the quench path A, one branch of the Fisher zeros $z_n(k)$ is seen to intersect with the imaginary axis in the complex time plane. However, for the quench paths B and C, the Fisher zeros $z_n(k)$ have no intersection with the imaginary axis. While for the quench path D, all two branches of Fisher zeros $z_n(k)$ will intersect with the imaginary axis. Meanwhile, for the quench paths A and D, we can find the corresponding cusp-like peaks of the rate functions at the critical times of the DQPTs [see Fig. 2(f)], which are in good agreement with the intersections between the Fisher zeros and the imaginary axis. However, for the quench paths B and C, the rate functions are smooth curves.

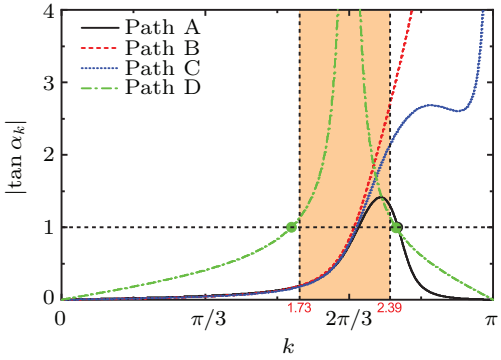


Fig. 3. Values of $|\tan\alpha_k|$ for the paths A, B, C, and D in Fig. 2(a), respectively. The orange block denotes the wave vectors k corresponding to $\varepsilon_k < 0$.

To understand the reason of the behavior of DQPT for the quench from the gapless phase, we draw $|\tan\alpha_k|$ as a function of k in Fig. 3 for the quench path A to D, respectively. The wave vectors interval $k \in (1.73, 2.39)$, in which $\varepsilon_k < 0$ of the pre-quench Hamiltonian $H(h_0 = 0.5, \gamma_0 = 0.2)$, is marked by the orange block. According to Eqs. (17) and (18), the DQPT will occur when $|\tan\alpha_k|$ reach 1 at the critical wave vectors outside the orange block. For the path A, it can be seen that there are two wave vectors satisfying $|\tan\alpha_k| = 1$, but one is inside the orange block and the other is outside. Therefore, there is one critical wave vector k^* of the DQPT in the quench path A. For paths B and C, the wave vectors for $|\tan\alpha_k| = 1$ are located in the orange block, so the DQPT can not occur for the quench paths B and C. While for the path D, there are two critical wave vectors k^* for $|\tan\alpha_{k^*}| = 1$ outside the orange block, which is exactly corresponding to two groups of DQPTs shown in Fig. 2(e). In summary, for the quench from the gapless phase, the occurrence of DQPT must satisfy the conditions (17) and (18) simultaneously.

3.2. Quench from the gapped phase

Now, we consider the case of quench from the gapped phase (FM phase and PM phase). It is found that the situation for the quench from the FM phase is essentially the same as that for the quench from the PM phase, so we take the case of quench from the FM phase as an example to discuss the behavior of DQPT in the quench from the gapped phase.

In Fig. 4(a), we display the domain $\mathcal{R}(h_0,\gamma_0)$ from the ground state of the pre-quench Hamiltonian $H(h_0=0.5,\gamma_0=-0.5)$, that is, from the FM$_y$ phase. It can be seen that the domain $\mathcal{R}(h_0=0.5,\gamma_0=-0.5)$ does not cover all the area of the CP phase, but cover all the area of the PM phase and the FM$_x$ phase. This indicates that the DQPT will always occur for the quench from the FM$_y$ phase to the PM phase and the FM$_x$ phase, but may not occur for the quench from the gapless CP phase. We find that the case of quench from the gapped phase to the gapped phase is similar to that in the XY chain,[6] so we focus on the case of quench from the gapped phase to the gapless phase.

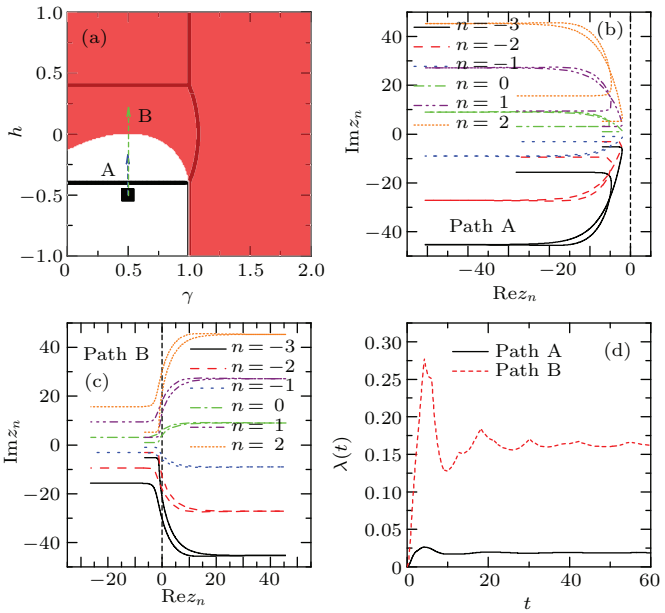


Fig. 4. (a) Domain $\mathcal{R}(h_0,\gamma_0)$ (the red region) for the quench from the FM phase. (b) and (c) Fisher zeros lines $z_n(k)$ for the quench paths A and B marked in (a). (d) Corresponding rate functions for the quench paths A and B.

We consider the case of quench from the FM phase to the gapless CP phase. As two examples, we show the Fisher zeros for the quench paths A and B in the Figs. 4(b) and 4(c), and the corresponding rate functions are shown in Fig. 4(d). Unlike the case of the quench from the gapless phase, the quasiparticle excitation spectra $\varepsilon_k>0$ for all the wave vectors k. Therefore, the Fisher zeros lines for the paths A and B are both continuous lines in the complex time plane. For the path A, the Fisher zeros are found having no intersection with imaginary axis [see Fig. 4(b)], and the rate function is the smooth function. There is no DQPT in the path A. However, for the path B, each Fisher zeros line $z_n(k)$ have two intersections with the imaginary axis. The corresponding critical times of DQPTs are seen as the cusp-like peeks of the rate function [see Fig. 4(d)].

Similarly, we show the values of $|\tan\alpha_k|$ for the quench paths A and B in Fig. 5. For the path A, all the values of $|\tan\alpha_k|$ are smaller than 1, so the DQPT can not occur because the condition (17) is not satisfied. However, for the path B, there are two critical wave vectors k^* for $|\tan\alpha_k|=1$, which is exactly corresponding to two intersections between each Fisher zeros line and the imaginary axis [see Fig. 4(c)]. Unlike the case of the quench from the gapless phase, the quasiparticle excitation spectra of the pre-quench Hamiltonian satisfy $\varepsilon_k>0$ for all the wave vectors k when the quench is from the gapped phase. Therefore, the occurrence of DQPT is actually determined by the condition (17).

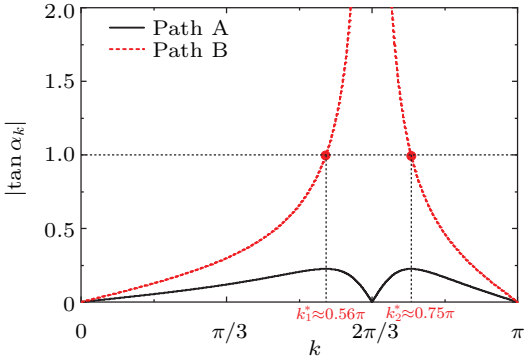


Fig. 5. Values of $|\tan\alpha_k|$ for the paths A and B in Fig. 4(a), which are from the FM to the CP phase.

4. The DQPT in the XY chain with three-site interaction

Now, we discuss the behavior of the DQPT in the XY chain with XZY–YZX type of three-site interaction.

4.1. Quench from the gapless CP phase

First, we consider the case of quench from the gapless CP phase. In Fig. 6(a), we show the domain $\mathcal{R}(0.5,0.1)$ which indicates that the DQPTs occur in the case of quench from the ground states of pre-quench Hamiltonian $H(0.5,0.1)$. It is found that the domain $\mathcal{R}(0.5,0.1)$ does not cover the area $h>1$, and leaves the blank blocks in the gapped FM$_x$ phase and FM$_y$ phase [see Fig. 6(a)]. This means that the DQPTs may not occur when the quench is from the ground state of $H(0.5,0.1)$ and across the QPTs. Similarly, we take four examples of the Fisher zeros for the quenches from gapless phase in Figs. 6(b)–6(e) corresponding to paths A–D in Fig. 6(a), and the rate functions are shown in Fig. 6(f). The Fisher zeros lines $z_n(k)$ in Figs. 6(b)–6(e) are found to be separated into two branches, because for some k the quasiparticle excitation spectra of the initial Hamiltonian satisfy $\varepsilon_k\cdot\varepsilon_{-k}<0$ [see Fig. 1(d)]. For the paths A and B in which the system is quenched to the covered area by domain $\mathcal{R}(0.5,0.1)$, the Fisher zeros lines have intersections with the imaginary axis, and the nonanalytic points can be seen in the rate functions. For the paths B and C, the Fisher zeros do not intersect with the imaginary axis, and the rate functions are seen to be smooth. At this moment, the DQPT does not occur even if the quench crosses the QPTs.

Similarly, we draw the values of $|\tan\alpha_k|$ in Fig. 7 for the paths A, B, C, and D to explain the occurrence and the absence of the DQPTs. It is found that the values of $|\tan\alpha_k|$

for all four paths have intersections with the line $|\tan\alpha_k| = 1$. However, for the paths B and C, the intersections are located in the orange block, where the wave vectors k do not contribute to the Fisher zeros. Therefore, the DQPTs do not occur in the quench paths B and C. For the paths A and D, the values of $|\tan\alpha_k|$ have one intersection outside the orange block. The corresponding wave vectors k^* of the intersections are exactly the critical wave vectors of the DQPTs.

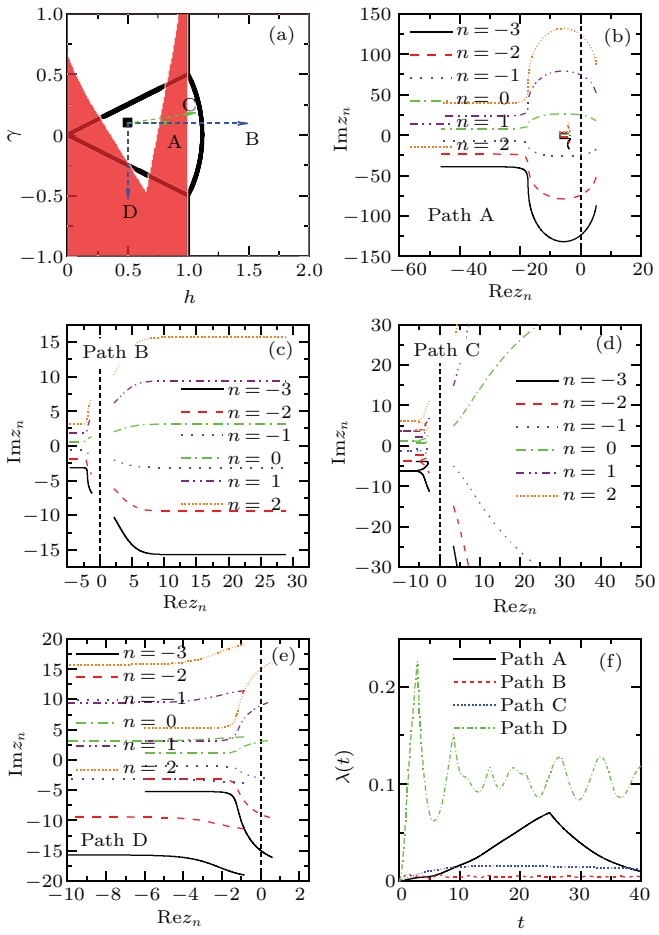


Fig. 6. (a) Domains $\mathcal{R}(h_0,\gamma_0)$ (the red region) for quench from the initial points (h_0,γ_0) in the XY chain with XZY–YZX type of three-site interaction. The initial point is $(h_0=0.5,\gamma_0=0.1)$. (b)–(e) The Fisher zeros for the quench paths A–D shown in (a). (f) The corresponding rate functions for the quench paths A–D.

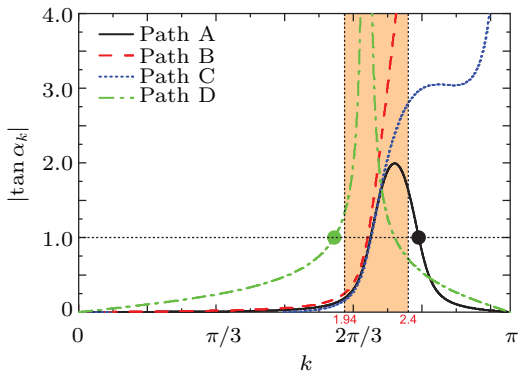


Fig. 7. Values of $|\tan\alpha_k|$ for the paths A, B, C, and D in Fig. 6(a), respectively. The orange block denotes the wave vectors k corresponding to $\varepsilon_k < 0$ of the pre-quench Hamiltonian.

4.2. Quench from the gapped phase

Now, we consider the case of quench from the gapped phase. Here we take the case of quench from the FM phase as an example. In Figs. 8(a), we show the domain $\mathcal{R}(h_0 = 0.5, \gamma_0 = -0.5)$ that is from the FM$_y$ phase. It is found that the domain $\mathcal{R}(h_0 = 0.5, \gamma_0 = -0.5)$ does not cover all the area of the gapless CP phase, but covers all the gapped phases which are not the initial points belonging to. This indicates that the DQPTs may not occur when the quench from the gapped phase to the gapless phase, but will always occur in the case of quench from the gapped phase to the gapped phase.

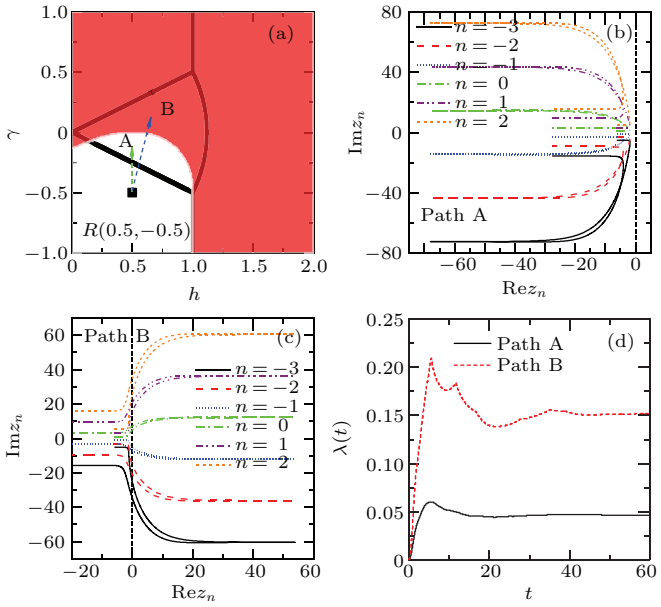


Fig. 8. (a) Domain $\mathcal{R}(h_0,\gamma_0)$ (the red region) for the quench from the FM phase. (b) and (c) Fisher zeros lines $z_n(k)$ for the quench paths A and B marked in (a). (d) Corresponding rate functions for the quench paths A and B.

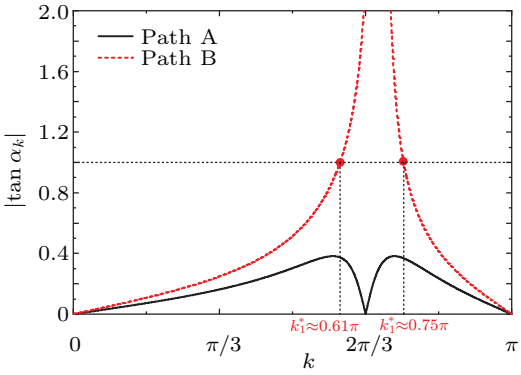


Fig. 9. Values of $|\tan\alpha_k|$ for the paths A and B in Fig. 8(a), which are from the FM to the CP phase.

As two examples, we show the Fisher zeros for the quench paths A and B marked in Fig. 8(a). It can be seen that for the quench path A, the Fisher zeros do not cross the imaginary axis. Meanwhile, the corresponding rate function is smooth. For the quench path B, each Fisher zeros lines $z_n(k)$ has two intersections with the imaginary axis, and the sharp peaks are seen in the rate function at the critical times of the DQPTs. Similarly, we display the values of $|\tan\alpha_k|$

for the paths A and B in Fig. 9. It is found that for the path A the values of $|\tan\alpha_k|$ are smaller than 1. However, for the path B the values of $|\tan\alpha_k|$ change from zero to the infinity ($|\tan\alpha_k| \in [0,+\infty)$) and have the intersections with the line $|\tan\alpha_k| = 1$.

5. Summary and conclusion

We study the properties of DQPTs in the XY chains with DM interaction and XZY–YZX type of three-site interaction, in which the systems have gapless phases and asymmetrical quasiparticle excitation spectra. By considering the quench starting from different initial states, we find that the factors $\mathcal{L}_k(t)$ of LE equal unity where the quasiparticle excitation spectra of pre-quench Hamiltonian satisfy $\varepsilon_k \cdot \varepsilon_{-k} < 0$. Therefore, we obtain the general conditions for the occurrence of DQPT, that is, the occurrence of DQPT not only requires the Bogoliubov angle to satisfy $|\tan\alpha_k| = 1$, but also requires the quasiparticle excitation spectra of the pre-quench Hamiltonian to satisfy $\varepsilon_k \cdot \varepsilon_{-k} \geq 0$.

Although we consider two specifical models in our paper, the conclusion can also be extended to a group of integral quantum spin chain, which can be mapped into the spinless free fermion model with the quadratic form by the Jordan–Wigner transformation. From the above discussion and the previous results,[22,27] we summarize the connection between the DQPT and the QPT as follows: For the system only with gapped phase, the DQPTs will occur when the quench crosses the critical lines of QPTs. For the system with the gapless phase, the DQPT may not occur in the quench from the gapped phase to the gapless phase or from the gapless phase to the gapped phase. For the systems with symmetrical quasiparticle excitation spectra, the reason for the absence of the DQPT is that there is no k satisfying $|\tan\alpha_k| = 1$. However, for the systems with asymmetrical quasiparticle excitation spectra, the reason for the absence of the DQPT is that no wave vector k satisfies $|\tan\alpha_k| = 1$, or the wave vectors k satisfying $|\tan\alpha_k| = 1$ correspond to $\varepsilon_k \cdot \varepsilon_{-k} < 0$.

Acknowledgement

This work was supported by the National Natural Science Foundation of China (Grant Nos. 11975126 and 11575087).

References

[1] Vojta T 2002 *Quantum Phase Transitions in Computational Statistical Physics* (Berlin: Springer) p. 211
[2] Sachdev S 2000 *Quantum Phase Transitions* (Cambridge: Cambridge University Press)
[3] Heyl M, Polkovnikov A and Kehrein S 2013 *Phys. Rev. Lett.* **110** 135704
[4] Karrasch C and Schuricht D 2013 *Phys. Rev. B* **87** 195104
[5] Hickey J M, Genway S and Garrahan J P 2017 *Phys. Rev. B* **89** 054301
[6] Vajna S and Dora B 2014 *Phys. Rev. B* **89** 161105
[7] Heyl M 2015 *Phys. Rev. Lett.* **115** 140502
[8] Vajna S and Dora B 2015 *Phys. Rev. B* **91** 155127
[9] Budich J C and Heyl M 2016 *Phys. Rev. B* **93** 085416
[10] Huang Z and Balatsky A V 2016 *Phys. Rev. Lett.* **117** 086416
[11] Zvyagin A A 2016 *Low Temp. Phys.* **42** 971
[12] Halimeh J C and Valentin Z S 2017 *Phys. Rev. B* **96** 134427
[13] Heyl M and Budich J C 2017 *Phys. Rev. B* **96** 180304
[14] Homrighausen I, Abeling N O, Valentin Z and Halimeh J C 2017 *Phys. Rev. B* **96** 104436
[15] Heyl M 2018 *Rep. Prog. Phys.* **81** 054001
[16] Cheraghi H and Mahdavifar S 2018 *J. Phys.: Conden. Matter* **30** 42LT01
[17] Wang P and Gao X 2018 *Phys. Rev. A* **97** 023627
[18] Yin H, Chen S, Gao X and Wang P 2018 *Phys. Rev. A* **97** 033624
[19] Zhou L, Wang Q, Wang H and Gong J 2018 *Phys. Rev. A* **98** 022129
[20] Lang H, Chen Y, Hong Q and Fan H 2018 *Phys. Rev. B* **98** 134310
[21] Huang Y P, Banerjee D and Heyl M 2019 *Phys. Rev. Lett.* **122** 250401
[22] Jafari R 2019 *Sci. Rep.* **9** 2871
[23] Liu T and Guo H 2019 *Phys. Rev. B* **99** 104307
[24] Yang K, Zhou L, Ma W, Kong X, Wang P, Qin X, Rong X, Wang Y, Shi F, Gong J and Du J 2019 *Phys. Rev. B* **100** 085308
[25] Chen S and Yang C 2019 *Acta Phys. Sin.* **68** 220304 (in Chinese)
[26] Deng T and Yi W 2019 *Acta Phys. Sin.* **68** 040303 (in Chinese)
[27] Haldar S, Roy S, Chanda T, Sen(De) A and Sen U 2020 *Phys. Rev. B* **101** 224304
[28] Cao K, Li W, Zhong M and Tong P 2020 *Phys. Rev. B* **102** 014207
[29] Hou X Y, Gao Q C, Guo H, He Y, Liu T and Chien C C 2020 *Phys. Rev. B* **102** 104305
[30] Zamani S, Jafari R and Langari A 2020 *Phys. Rev. B* **102** 144306
[31] Fu H, Cao K, Zhong M and Tong P 2021 *Acta Phys. Sin.* **70** 480502 (in Chinese)
[32] Jurcevic P, Shen H, Hauke P, Maier C, Brydges T, Hempel C, Lanyon B P, Heyl M, Blatt R and Roos C F 2017 *Phys. Rev. Lett.* **119** 080501
[33] Zhang J, Pagano G, Hess P W, Kyprianidis A, Becker P, Kaplan H, Gorshkov A V, Gong Z X and Monroe C 2017 *Nature* **551** 601
[34] Wang K, Qiu X, Xiao L, Zhan X, Bian Z, Yi W and Xue P 2019 *Phys. Rev. Lett.* **122** 020501
[35] Nie X, Wei B B, Chen X, Zhang Z, Zhao X, Qiu C, Tian Yu, Ji Y, Xin T, Lu D and Li J 2020 *Phys. Rev. Lett.* **124** 250601
[36] Tian T, Yang H X, Qiu L Y, Liang H Y, Yang Y B, Xu Y and Duan L M 2020 *Phys. Rev. Lett.* **124** 043001
[37] Xu X Y, Wang Q Q, Heyl M, Budich J C, Pan W W, Chen Z, Munsif J, Sun K, Xu J S, Han Y J, Li C F and Guo G C 2020 *Light: Sci. Appl.* **9** 7
[38] Dzyaloshinsky I 1958 *J. Phys. Chem. Solids* **4** 241
[39] Moriya T 1960 *Phys. Rev. Lett.* **4** 228
[40] Derzhko O and Richter J 1999 *Phys. Rev. B* **59** 100
[41] Yang J, Li J, Lin L and Zhu J J 2020 *Chin. Phys. Lett.* **37** 087501
[42] Krokhmalskii T, Derzhko O, Stolze J and Verkholyak T 2008 *Phys. Rev. B* **77** 174404
[43] Gottlieb D and Rossler J 1999 *Phys. Rev. B* **60** 9232
[44] Kitaev A 2006 *Ann. Phys.* **321** 2
[45] Rodney M, Song H F, Lee S S, Le H K and Srensen E S 2013 *Phys. Rev. B* **87** 115132
[46] Suzuki S, Inoue J, and Chakrabarti B K 2013 *Transverse Ising Chain (Pure System) in Quantum Ising Phases and Transitions in Transverse Ising Models* (Berlin: Springer)) p. 13
[47] Zhong M, Xu H, Liu X X and Tong P 2013 *Chin. Phys. B* **22** 090313
[48] Liu X, Zhong M, Xu H and Tong P 2012 *J. Stat. Mech.* **2012** P01003